JOURNAL OF APPLIED ELECTROCHEMISTRY **24** (1994) 95–106

Studies of three-dimensional electrodes in the FM01-LC laboratory electrolyser

C. J. BROWN, D. PLETCHER

Department of Chemistry, University of Southampton, Southampton SO9 5NH, Great Britain

F. C. WALSH

Department of Chemistry, University of Portsmouth, Portsmouth PO1 2DT, Great Britain

J. K. HAMMOND, D. ROBINSON

ICI Chemicals & Polymers Limited, Research and Development Department, PO Box 8, The Heath, Runcorn, Cheshire WA7 4QD, Great Britain

Received 17 February 1993; revised 2 July 1993

A FM01-LC parallel plate, laboratory electrochemical reactor has been modified by the incorporation of stationary, flow-by, three-dimensional electrodes which fill an electrolyte compartment. The performance of several electrode configurations including stacked nets, stacked expanded metal grids and a metal foam (all nickel) is compared by (i) determining the limiting currents for a mass transport controlled reaction, the reduction of ferricyanide in 1 M KOH and (ii) measuring the limiting currents for a kinetically controlled reaction, the oxidation of alcohols in aqueous base. It is shown that the combination of the data may be used to estimate the mass transfer coefficient, k_L, and the specific electrode area, A_e, separately. It is also confirmed that the use of three dimensional electrodes leads to an increase in cell current by a factor up to one hundred. Finally, it is also shown that the FM01-LC reactor fitted with a nickel foam anode allows a convenient laboratory conversion of alcohols to carboxylic acids; these reactions are of synthetic interest but their application has previously been restricted by the low rate of conversion at planar nickel anodes.

Nomenclature

A_e	electrode area per unit electrode volume ($m^2\,m^{-3}$)
c	bulk concentration of reactant ($mol\,m^{-3}$)
E	electrode potential vs SCE (V)
$E_{1/2}$	half wave potential (V)
F	Faraday constant ($96\,485\,C\,mol^{-1}$)
I	current (A)
I_L	limiting current (A)
j_L	limiting current density ($A\,m^{-2}$)
k_L	mass transfer coefficient ($m\,s^{-1}$)
n	number of electrons transferred
p	empirical constant in Equation 2
ΔP	pressure drop over reactor (Pa)
R	resistance between the tip of the Luggin capillary and the electrode surface (Ω)
q	velocity exponent in Equation 2
v	(interstitial) linear flow rate of electrolyte ($m\,s^{-1}$)
V_e	volume of electrode (m^3)

1. Introduction

It is widely recognized that the rate of conversion within an electrochemical reactor can be increased substantially by the use of a three dimensional electrode and the properties of such electrodes have been extensively reviewed [1–8]. It is generally accepted that three-dimensional electrodes are particularly appropriate when the rate of conversion is low and limited either by the low concentration of reactant or a slow chemical step. There are, however, limitations on the design and scaling of three-dimensional electrodes. Potential drop through the solution phase within the porous electrode may lead to an uneven potential distribution which will limit the useful thickness of the three dimensional electrode especially when the reactant concentration is high or the electrolyte medium is poorly conducting. The current distribution can be affected by local variations in the mass transport regime and depletion of the reactant as well as being determined by the potential distribution. Even the space averaged current density depends on the exact choice of the material for the electrode through the extent to which it acts as a turbulence promoter and its specific surface area. Certainly, the performance of practical three dimensional electrodes cannot readily be predicted from theoretical considerations and it is therefore essential to determine, by experiment, the optimum

0021-891X

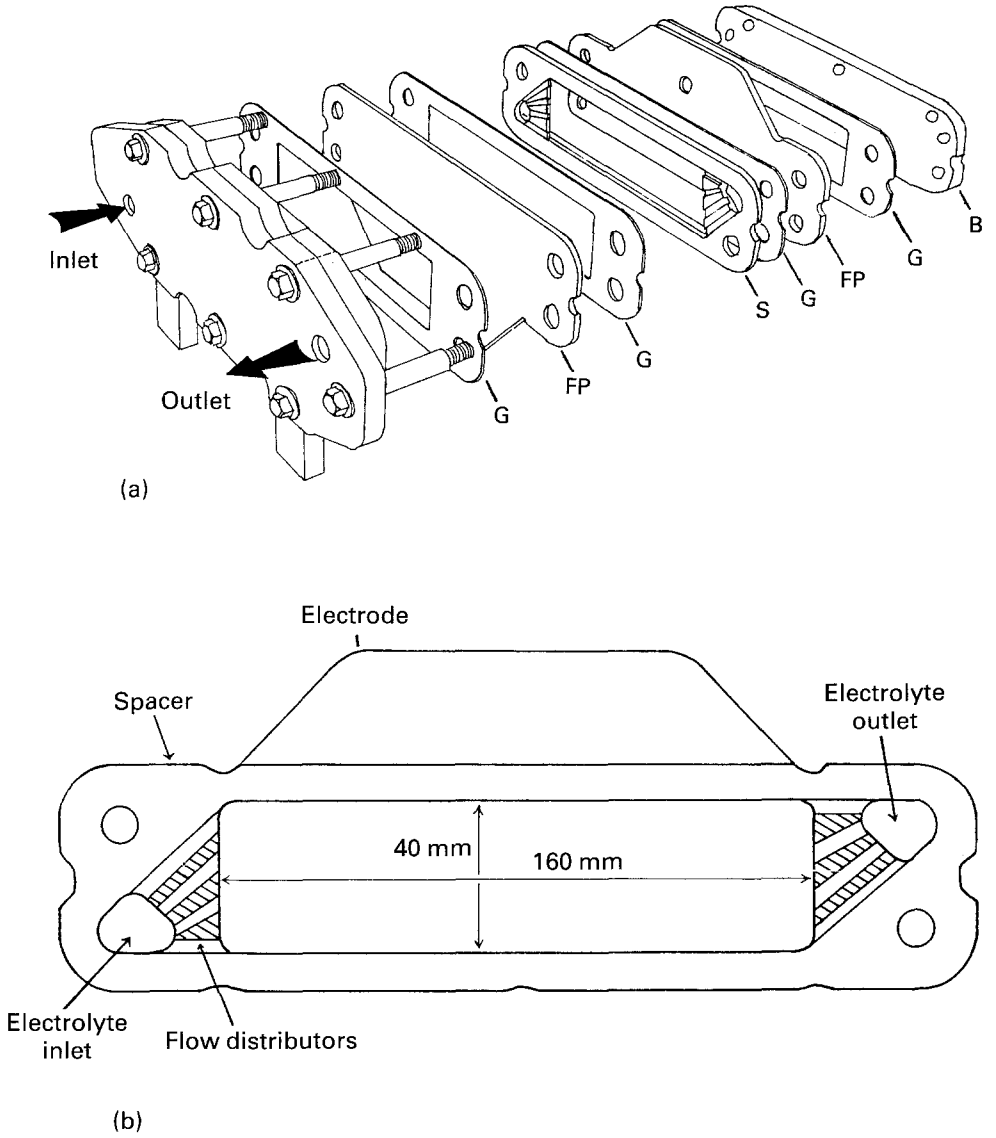

Fig. 1. (a) Exploded view of the FM01-LC reactor in the undivided mode with one electrode pair separated by two gaskets and one spacer. (B) Backplate, (G) gasket, (S) spacer, and (FP) flat plate. (b) Plan view of a flat plate electrode with a spacer in place showing the electrolyte channel and flow distributors. The three dimensional electrodes were designed to fill the electrolyte chamber within the spacer.

electrode structure as well as its maximum useful dimensions.

It is often convenient to construct cells with a stationary, flow-by, three dimensional electrode simply by the modification of a parallel plate reactor. It is then only necessary to fabricate (from a porous conducting material) an electrode to fill one electrolyte compartment and the flat plate electrode may then be used as a current collector. This approach, for example, has been used to modify both laboratory cells [9] and commercial cells, eg. Electro-Syn and ElectroProd cells (marketed by ElectroCell AB) [10]. In this paper we describe the study and operation of a variety of three dimensional nickel electrodes in the FM01-LC electrolyser (marketed by ICI Chemicals & Polymers Ltd). Figure 1 shows an exploded view of this reactor as well as a plan view of a flat plate electrode and spacer (which also defines the electrolyte chamber and incorporates the electrolyte distributors). A fuller description of this electrolyser is available [11] while earlier papers by the present authors have discussed space averaged mass transport at plate electrodes with/without turbulence promoters [12, 13] as well as investigations of the local variations in the mass transport regime [14]. The experiments reported here sought to determine (i) space averaged mass transport characteristics for several types of three dimensional nickel materials and (ii) cell currents when there is no mass transport limitation and the current is determined only by the rate of a chemical reaction at the nickel surface. The latter experiments offer an alternative approach to the interpretation of data from pressure drop versus flow rate measurements for the separate determination of the mass transfer coefficient, k_L, and specific surface area, A_e. The experiments employed the oxidation of ethanol at a nickel oxide anode in aqueous base, a reaction well understood at two dimensional electrodes [15–18]. Finally, it is shown that the FM01-LC cell with a nickel foam anode is an excellent cell for the conversion of alcohols to carboxylic acids and may be used to

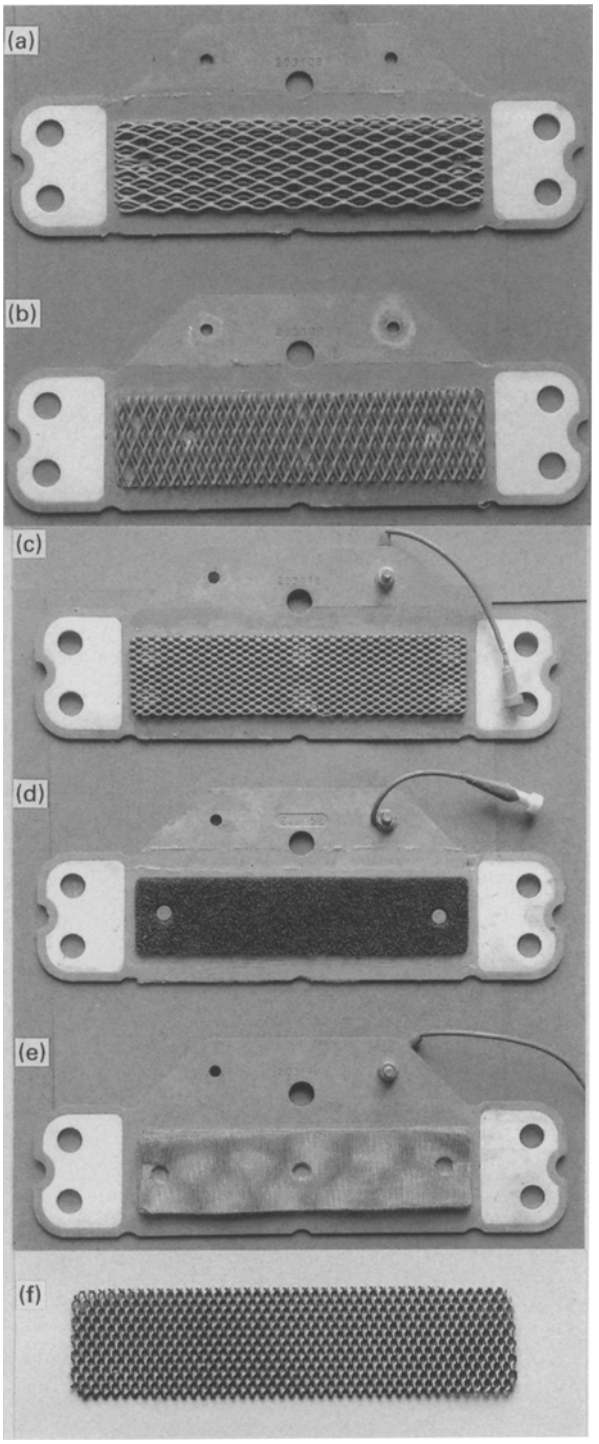

Fig. 2. Photographs of the three-dimensional, nickel electrodes. (a) EXP L (b) EXP S (c) twin grid (d) metal foam (e) stacked nets (f) stacked grids.

facilitate the electrosynthesis of a polyfunctional carboxylic acid.

2. Experimental details

2.1. *Equipment*

Most of the electrochemical experiments were carried out using a HiTek potentiostat, model DT2101, and waveform generator, model PPR1. Current–potential curves were recorded on a Gould 60000 series chart recorder. Constant current electrolyses were carried out using a Powerline, model LAB 502 power supply. Charge was measured using a digital integrator, built 'in-house'. All potentials in this paper were measured against a Radiometer type K401 saturated calomel electrode.

2.2. *Cells*

Details of the flow circuit and pressure drop measurements [12] as well as the FM01-LC electrochemical

reactor [11] are given in earlier publications. All electrodes in this study were fabricated from nickel materials (including the counter electrode which was always a flat nickel plate). In one of its standard configurations, the cell has two flat plate electrodes each with an active area 16 cm × 4 cm. Several three-dimensional electrodes were used in this study, see Fig. 2, and the geometrical characteristics of the electrodes are reported in Table 1. Most of the nickel materials were obtained from the Expanded Metal Company: EXP S and EXP L were fabricated from expanded nickel type 197V and 197H, respectively, the twin grid TWB from type TWB-H and the stacked net electrode from a fine nickel mesh, type 976. The foam was Retimet^{TM} 45 (45 p.p.i.) supplied by Dunlop Aviation Ltd. Generally, the three dimensional electrodes were fabricated so as to fill the electrolyte chamber within the spacer so that their area parallel to the counter electrode was 16 cm × 4 cm. In a few cases, the overall dimensions of the three-dimensional electrodes were slightly less and then, to avoid bypassing of the electrolyte, strips of silicone rubber were placed along the top and bottom edges of the electrodes. The normal depth of the electrodes are listed in Table 1. For particular purposes, the depth of the electrodes were varied, and in such cases the number of spacers and gaskets which made up the electrolyte channel were adjusted accordingly. When operating in the undivided mode, electrical shorting between the working and counter electrodes was prevented by placing one or more pieces of polypropylene mesh between them. A few experiments used a smaller foam metal electrode; this was 2 cm (in the direction of flow) × 4 cm (across the flow) × 3 mm (deep) and was placed at the centre of the electrolyte chamber with plastic meshes on either side. Divided cell experiments were carried out with a Nafion^{TM} 324 cation permeable membrane separating the compartments. For controlled potential experiments, a capillary tube was inserted through the wall of the spacer to act as a Luggin capillary. All mean linear flow velocities were corrected for the differences in the cell configuration and the volumes of the electrode materials (i.e. the stated values are interstitial velocities).

The current distribution through the depth of a stack of nickel grids was investigated using four grids, measuring 15.5 m × 4 cm, made from material supplied by the Expanded Metal Company (type 226F); its geometrical characteristics are shown in Table 1. The grids were electrically insulated by spacers of polypropylene mesh (mesh size 1 mm). Electrical contacts were made by spot welding two insulated nickel wires (0.25 mm diameter) along the trailing edge of the electrode, the wires being inserted through the polymer gasket using silicone rubber to prevent electrolyte leakage. The cell was used in the undivided mode with a nickel flat plate counter electrode. The counter electrode was separated from the fourth grid in the stack, again by a polypropylene mesh. The total cell depth with this arrangement was 0.75 cm. Current measurements at an individual grid was made whilst the remaining grids were active and still passing current. This was made possible by using a four-way make-before-break switch, which enabled the current follower of the potentiostat to switch between each grid without interrupting the current flow from any of them. Potential control of the electrode was achieved in a similar manner to that of the previous experiments, with a Luggin capillary passing through a cell wall spacer and situated between the second and third grid.

Voltammograms were recorded at a nickel disc electrode, area 0.20 cm^2, made by sealing a nickel rod into a glass tube with epoxy resin. The experiments used a three-electrode, two-compartment glass cell of standard design.

2.3. *Chemicals and procedures*

The electrolytes were prepared with water from a Millipore purification system and the chemicals were Analar or the highest available grade and were used without purification. The electrolyte for the mass transport studies was 0.1 to 5×10^{-3} M potassium ferricyanide plus at least a fourfold excess of potassium ferrocyanide in 1 M potassium hydroxide. For the study of their oxidation, various concentrations of the alcohols were employed, all in 1 M potassium hydroxide. All experiments were carried out at 298 K after the solutions were thoroughly deoxygenated with a fast stream of nitrogen. *I–E* curves were recorded with a potential scan rate of 3 mV s^{-1}. Electrolyte flow rates were varied over a mean linear velocity range of 1 to 15 cm s^{-1}.

Disc electrodes were highly polished using various grades of alumina down to 0.5 μm powder on a polishing cloth. The plate electrode was prepared using 600 then 1200 grade emery paper before being degreased with acetone and washed thoroughly with distilled water. Clearly, physical pretreatment of the three dimensional electrodes was practically impossible. All electrodes were, however, pretreated electrochemically in 1 M potassium hydroxide before use. When used as a cathode, the electrodes were allowed to evolve hydrogen for 1200 s in order to ensure complete removal of oxides; with the flat plate the current density was 10 mA cm^{-2} (total cell current 0.64 A) and with the three-dimensional electrodes, the cell current was 1.28 A, giving a superficial current density of 20 mA cm^{-2}. When used as anodes the potential was cycled between +0.3 V and +0.5 V at 1 mV s^{-1} for one hour, thereby ensuring a more reproducible oxide coating.

2.4. *Analysis*

The consumption of alcohols was followed by gas chromatography of samples taken from the anolyte.

Table 1. Characteristics of the extended area electrodes

Electrode type	*Number*	*CD** /mm	*LD** /mm	*Orientation to flow*	*Strand width* /mm	*Strand thickness* /mm	*Bed depth* /mm	*Electrode volume* /cm^3	*Porosity*†
EXP S	2	3.5	10.5	CD	1.33	0.7	3.5	20.7	0.70
EXP L	2	3.5	10.5	LD	1.33	0.7	3.5	20.7	0.70
Twin grid	2	1.75	3.0	LD	1.0	1.0	4.0	20.7	0.56
Stacked net	30	1.02	1.50	LD	0.13	0.13	5	27.9	0.68
Metal foam§	1	N/A	N/A	N/A	N/A	N/A	4.0	22.3	0.87
Stacked grid‡	4	1.4	3.0	CD	1.0	1.25	7.5	–	0.62

* The CD and LD are the lengths of the short and long dimensions respectively of the grid/net.
† Porosity equates to the ratio of free volume in the channel to the overall channel volume.
‡ Only used for experiment on current distribution.
§ Graded as 45 pores per linear inch.

Gas chromatography was carried out with either (a) a Perkin Elmer model 8310 gas chromatograph using a 12.5 m BP/1 capillary column or (b) a Varian model 3700 packed column gas chromatograph, with a 2 m Porapak Q column. The yields of carboxylic acid products were determined by (i) removing, at regular intervals during an electrolysis, a 2.5 cm^3 aliquot of the electrolyte (ii) loading the sample onto an ion exchange column (Amberlite 120-H in its H^+ form) and eluting with distilled water (iii) titrating the eluent with a standard 0.01 M solution of sodium hydroxide. The product identity was also checked using gas chromatography by comparing the retention time of the product with that of a commercial sample. Infrared spectra were obtained using a Perkin Elmer, model 298 spectrometer and NMR were recorded on a Bruker Aspect 3000 spectrometer.

3. Results and discussion

3.1. *Characterization of mass transport*

Current–potential curves were recorded for a solution of ferricyanide in 1 M KOH at each of the nickel electrodes for a series of mean linear electrolyte flow rates. In each case, the potential was scanned from the rest potential (+0.20 V) to −1.10 V vs SCE at a scan rate of 3 mV s^{-1}. Due to the large differences in the current responses from the different electrodes, the concentration of ferricyanide ion was varied so that the cell current fell in the range 0.1–1.0 A for all flow rates employed. For experiments with the EXP S and EXP L expanded metal, TWB twin grid and flat plate electrodes, the solution contained 5.0×10^{-3} M ferricyanide but for the metal foam and stacked net electrode, the ferricyanide concentration was $(0.1–1.0) \times 10^{-3}$ M. All solutions contained a 4–20 fold excess of ferrocyanide, sufficient to ensure that the only anode reaction was the regeneration of ferricyanide. With an appropriate concentration of reactant, well formed reduction waves with limiting plateaux extending over 0.7 V were observed with all of the electrodes. The limiting currents, I_L, were measured at a potential of −0.4 V. Figure 3 shows plots of I_L/c as a function of the mean linear flow rate, v, of the electrolyte for each of the three-dimensional electrodes as well as a flat plate cathode. Each point on this graph is an average based on five separate measurements of the limiting current whose values varied less than 3%. It can be seen that the mass transport limited currents normalised for reactant concentration (i.e. I_L/c) at the different electrodes vary strongly and in the case of the stacked net, the current response is approximately one hundred times that at the flat plate.

Since the reduction of ferricyanide at nickel is mass transport controlled and calculation shows that the conversion through the cell is less than 5%, the

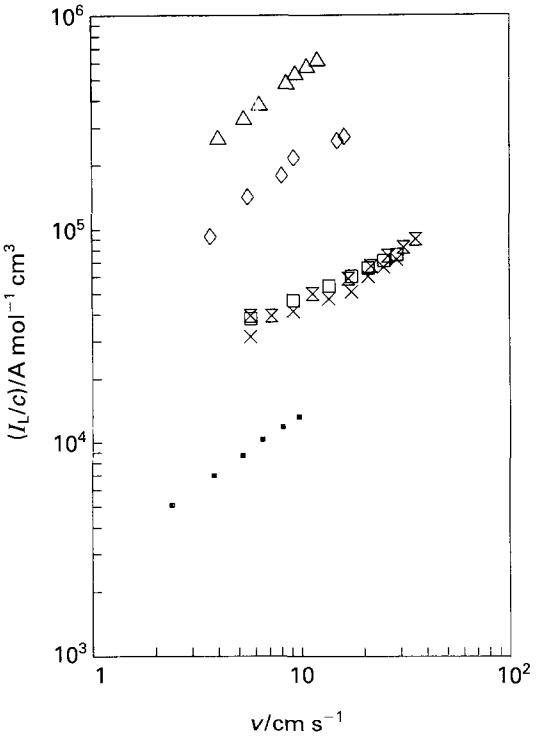

Fig. 3. Limiting currents normalised for reactant concentration as a function of mean linear flow for a flat plate and several three-dimensional, nickel electrodes. The mean linear flow velocities are corrected for the slightly different cell configurations and the volumes of the electrode materials. The solutions were $(0.1–5.0) \times 10^{-3}$ M $Fe(CN)_6^{3-}$ in 1 M KOH with a 4–20 fold excess of $Fe(CN)_6^{4-}$. Key: (△) stacked net; (◇) metal foam; (⊠) twin grid; (□) EXP S; (×) EXP L; (•) flat plate.

data were used to calculate values of $k_L A_e$ using the equation

$$I_L = nFV_e k_L A_e c \quad (1)$$

where V_e is the volume of the electrode, k_L the mass transfer coefficient and A_e the specific surface area of the nickel material. The values of $k_L A_e$ as a function of linear flow rate were then fitted to equations of the type

$$k_L A_e = pv^q \quad (2)$$

where p and q are empirical constants. Table 2 reports values for each of the nickel materials. The experiments employed Reynolds numbers in the range 200–2000 and the values of q clearly indicate that the flow within the cell is always at least partially turbulent. This is not surprising since, even with a flat plate electrode, the exponent for the linear flow rate is 0.70, well above the value of 0.33 expected for fully developed laminar flow [13]. Indeed, a trend observed with this cell is that several of the three-dimensional materials (as well as turbulence promoters with similar structures [13]) lead to a lower value of the exponent, perhaps arising from some laminization of the flow. With the stacked net electrode, the flow appears to be fully turbulent while the value of q for the metal foam is also high. The values of p compare the parameter, $k_L A_e$, at one flow rate. While it is clear that much of the variation results from differences in specific surface areas, there is clearly also a contribution from the differences in the mass transport regimes with the various nickel materials. This is more clearly seen if the comparison of $k_L A_e$ is made at higher flow rates. Another example of a mass transport effect may be seen by comparing the two expanded metal electrodes, EXP S and EXP L. These electrodes are made from the same material and have the same areas. They differ only in the orientation of the lattice to the direction of electrolyte flow. At all flow rates EXP S gives a higher current than EXP L, typically by some 20%. It is interesting to note that using two 'expanded' polymer turbulence promoters with similar geometrical patterns, type B and C in an earlier paper [13], led to the same trend in currents at a flat plate electrode. Hence, whether it acts as an electrode or a plastic mesh turbulence promoter, the structure with the long diagonal at right angles to the electrolyte flow produces a greater degree of localized turbulence because the flow meets an obstacle more frequently. The results for the EXP S and EXP L expanded metal electrodes are also comparable with those obtained by Leroux and Coeuret [19] who studied expanded materials of a similar design in a flow-by configuration. These authors found the short diagonal arrangement gave an increase in mass transport by a factor of 1.4 over that of the long diagonal arrangement. It should also be noted that the values of $k_L A_e$ reported above for the 45 p.p.i. nickel foam are the same magnitude as those reported by Langlois and Coeuret [20]. The value of the exponent of the linear flow velocity, q, is, however, quite different. Langlois and Coeuret [20] obtained $q = 0.47$ while we have found the value $q = 0.70$. It must be remembered, however, that the cell designs are quite different; in particular, our cell design does not have a calming zone at the entry and exit to the electrolyte chamber. Hence, it should be recognised that the correlation equations will depend on the many factors in the cell design; they are not a property of the three-dimensional electrode alone.

Table 2. Data from the measurements of the mass transport limiting currents for the reduction of ferricyanide in 1 M KOH at various three-dimensional nickel electrodes presented as correlations to $k_L A_e = pv^q$ where v has the units of cm s^{-1}. The quantity r is the linear correlation factor

	$10^2 p$	q	r
EXP S	0.95	0.41	0.998
EXP L	0.66	0.50	0.996
Twin grid	0.72	0.51	0.999
Stacked net	3.24	0.80	0.999
Metal foam	1.89	0.70	0.988

3.2. *Pressure drop measurements*

Pressure drops were determined across each of the electrode materials. In the experiments reported here, the measurements were made with pressure taps exterior to the cell and within the electrolyte inlet and outlet pipes so as to include the pressure drop within the electrolyte inlet and outlet manifolds to the cell. The presence of the three dimensional electrode structures within the electrolyte compartment increased the pressure drop by less than 20%. This was also the case when the electrolyte channel was filled with turbulence promoters [13]. More detailed pressure drop measurements will be presented in a later paper.

3.3. *Current distribution perpendicular to the electrolyte flow*

Clearly, the current distribution perpendicular to the solution flow is critical to the performance of a three dimensional electrode in a flow-by cell and determines the useful electrode depth. Therefore a few experiments were carried out to determine this current distribution using a stack of four, electrically insulated nickel grids. In the results presented here, the grid numbering is 1 for the grid nearest the backplate and 4 for that closest to the counter electrode. Current–potential responses were recorded at each of the grids while the whole stack is active for a series of flow rates of a solution which is 1×10^{-3} M ferricyanide and 20×10^{-3} ferrocyanide in 1.0 M KOH. A set of curves at one flow rate (7.2 cm s^{-1}) are shown in Fig. 4(a). It can be seen that, at all grids, the I–E response rises steeply from the equilibrium potential and reaches a limiting current plateau which extends over 0.8 V. Moreover, the limiting currents observed depend strongly on the linear flow rate, confirming

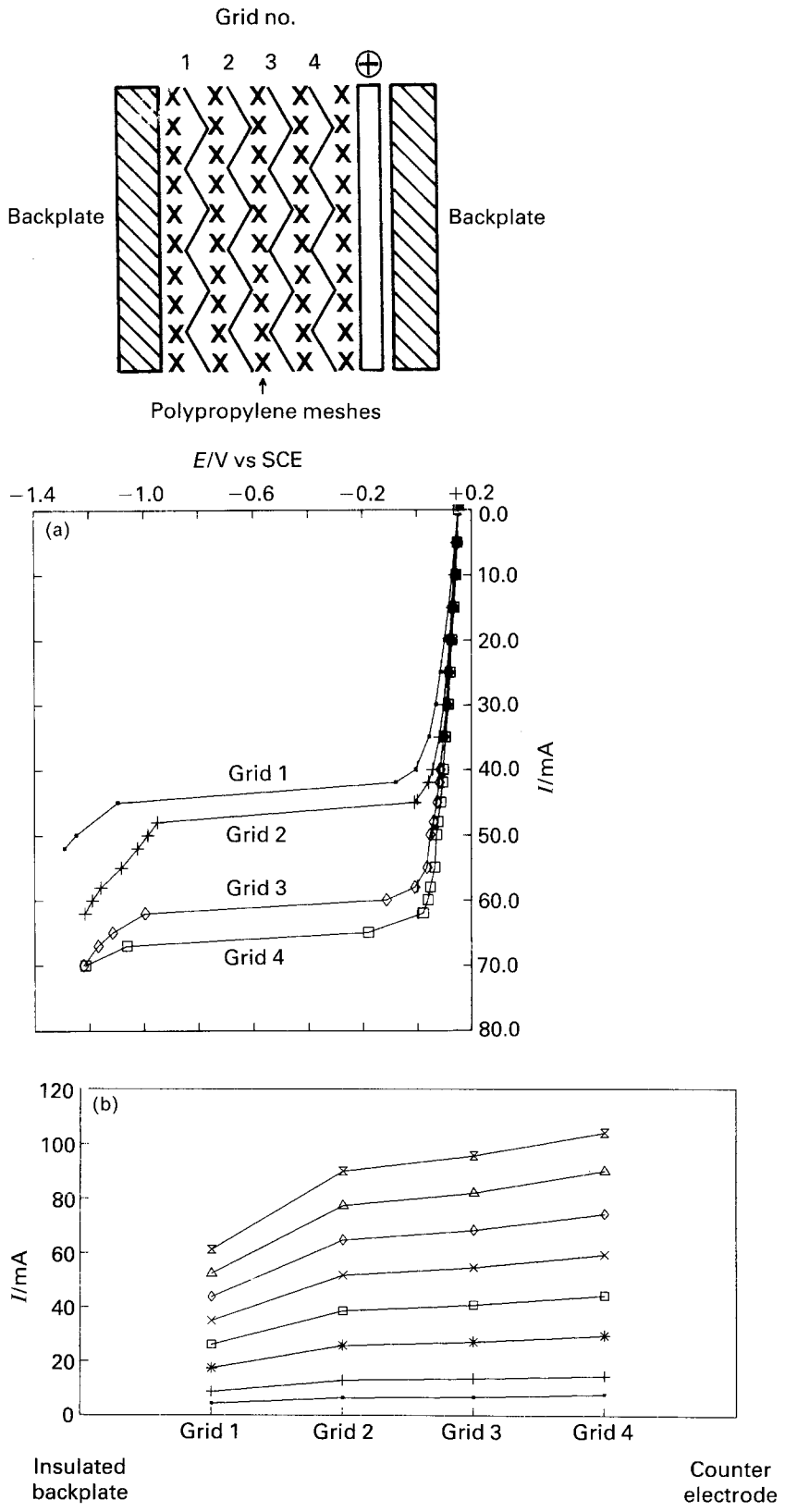

Fig. 4. (a) I–E curves for the reduction of 1×10^{-3} M $Fe(CN)_6^{3-}$ in 1 M KOH at each grid of a stack of four grids. All grids are active during the recording of the curves. (b) Currents at each of the grids when the cell is operating at a constant current density. Total cell current: (⧖) 350; (△) 300; (◇) 250; (×) 200; (□) 150; (*) 100; (+) 50 and (●) 25 mA.

that they are determined by convective-diffusion mass transport. The experiments were repeated with a five-fold increase in $Fe(CN)_6^{3-}$ concentration, when the total cell current is in excess of 1 A, but the shapes of the I–E curves were unchanged (further increases in reactant concentration were not possible because of instrumentation limitations). The results were, however, confirmed by a second series of experiments where the total cell current was controlled at various values (between ~ 2% and ~ 40% of the mass transport controlled current) and the currents to the individual electrodes measured. These results are shown in Fig. 4(b). It can be seen that at low cell currents (in the region of electron transfer control) there is no current variation, but with increasing cell current (as the system moves into partial mass transport control), the variation in current between the four grids is clearly seen.

Table 3. Slopes of plots of limiting current densities against concentration of three alcohols for different nickel electrodes

	Slopes of j_L against c plots† */A cm mol*$^{-1}$		
	Disc	*Flat plate*	*Metal foam**
ethanol	9.1	6.0	650
propanol	5.3	–	310
butanol	1.2	–	77

* measured at 0.44 V vs SCE: based on area of back plate.
† these slopes are proportional to the rates of Reaction 4.

Hence, there is no evidence of a significant potential drop through the stack in these conditions with cell currents of 1 A. On the other hand, it is apparent that the limiting currents at the four grids are different and this variation is more pronounced at higher flow rates. Therefore, the local mass transport regimes are not the same at the four grids and the grids nearest the backplate see a significantly lower rate of mass transport. Further experiments were carried out where the arrangement of the spacers and gaskets was altered so as to move the solution inlet and outlet with respect to the grid positions. This did not cause a significant change to the limiting currents and it is concluded that the local mass transport regimes arise from the proximity of cell structural features such as the backplate and not the electrolyte distribution. It is also concluded that the FM01 cell can be used with three dimensional electrodes without fear of a significant potential drop. More generally, it should be noted that the electrodes are relatively thin and the experiments also use a highly conducting aqueous media. Leroux and Coeuret have reported the potential distribution through a stack of nets in a flow-by cell using a moveable potential probe [21]. Using similar solutions to ourselves, they also found small potential drops generally below 100 mV when the cell was operating in the mass transport controlled regime. Their technique is certainly more sensitive to small potential distributions but is difficult to implement in practical cells. In this respect, there does not appear to be significant differences in the conclusions from the studies. The same workers [19] also determined the current distribution and, in the mass transport controlled plateau, found no variation with grid position. This must again be interpreted in terms of the quite different cell configurations.

3.4. *Oxidation of alcohols*

As noted above, these experiments were carried out with two different objectives: (i) the measurement of the currents for a reaction fully controlled by the kinetics of a surface reaction offers a potential way to determine specific surface areas for the materials and (ii) the use of extended area electrodes would appear to be a way to carry out these reactions on a synthetic scale and at a useful rate.

Slow scan voltammograms for the oxidation of ethanol in 1 M KOH at a highly polished nickel disc electrode were recorded and Fig. 5 shows a set of curves for several concentrations of ethanol. It can be seen that well-shaped oxidation waves with clearly defined limiting current plateaux are observed with $E_{1/2} \sim 0.39$ V vs SCE. Oxygen evolution is seen to commence at +0.46 V. The potential range where ethanol is oxidised coincides with that for the oxidation of nickel(II) hydroxide on the surface of the electrode (formed as soon as the nickel contacts the KOH solution) to an oxide/hydroxide with the nickel in a higher oxidation state. It may also be noted that although the limiting current densities are proportional to the ethanol concentration (see inset to Fig. 5), they also occur at much lower current densities than expected for mass transport controlled $4e^-$ oxidation (the product is known to be ethanoic acid [15, 18]). These data are entirely consistent with the literature [15–18] and the following, accepted mechanism.

$$Ni(OH)_2 + OH^- - e^- \rightarrow NiO(OH) + H_2O \quad (3)$$

$$NiO(OH) + RCH_2OH \rightarrow Ni(OH)_2 + RCH^{\cdot}OH \quad (4)$$

$$RCH^{\cdot}OH + 3OH^- - 3e^- \rightarrow RCOOH + 2H_2O \quad (5)$$

where the surface chemical reaction, Step 4, is the rate determining step. Experiments with propanol and ethanol gave similar responses although the limiting current densities are lower (see Table 3), reflecting the slower rates of Reaction 4 for these alcohols.

Current–potential curves were also recorded at a flat plate nickel electrode in the FM01 cell for solutions of ethanol (concentrations 5–50 mM) in 1 M KOH. The responses again showed oxidation waves at ~ 0.39 V; the limiting current plateaux, although clearly visible, were also slightly less well defined than at the nickel disc electrodes. The limiting currents were measured at 0.43 V and their values vary linearly with ethanol concentration. The slope of the j_L against c plot (Table 3) is, however, less than that at the nickel disc. We believe that this reflects a different catalytic activity of the two nickel surfaces. It has previously been noted that the rate of the alcohol oxidations on the nickel hydroxide layer depends strongly on the history, pretreatment and composition of the nickel surface. The trend found is, however, the opposite to that expected on the basis of the surface roughnesses. The disc, after extensive polishing, was highly reflecting, while even after preparation, the nickel plate still has a comparatively dull and matt appearance and clearly had a rougher surface.

The studies were extended to the three dimensional electrodes. All three alcohols were studied at the nickel foam anode of reduced size (a piece of nickel foam 2 cm × 4 cm, placed at the centre of the electrolyte path through the reactor). A set of I–E curves for ethanol is shown in Fig. 6. At the three dimensional

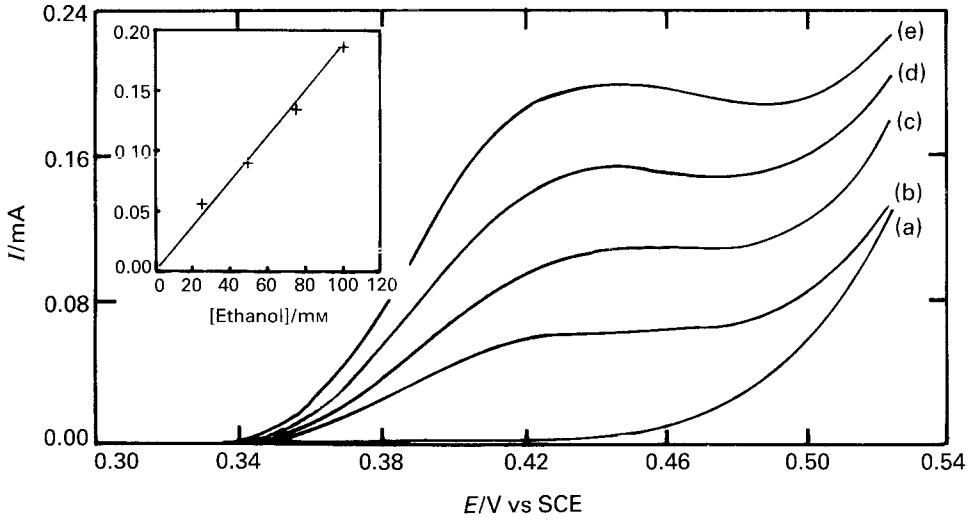

Fig. 5. I–E curves for ethanol in 1 M KOH at a polished nickel disc. Potential scan rate 1 mV s^{-1}. Ethanol concentrations: (a) 0; (b) 25; (c) 50; (d) 75; and (e) 100 mM. The inset shows the relationship between I_L and the concentration of ethanol.

material, it is difficult to identify the limiting current plateaux although the current in the presence of ethanol is well above the background level and the anodic current is being observed in the expected potential range. The limiting currents were therefore estimated by measuring the currents at +0.44 V and subtracting the current at this potential in the absence of any organic. The 'limiting currents' are again proportional to the ethanol concentration. The value of the slope of the j_L against c plot as well as those for similar sets of experiments with propanol and butanol are reported in Table 3. It can be seen that the ratio of the slopes of the j_L against c plots for the three alcohols at the highly polished nickel disc and the nickel foam are very similar. This is to be expected since the ratio of j_L/c is expected to depend only on the relative areas of nickel exposed to solution and their relative activities. It should be emphasized that the value of j_L/c for a mass transfer controlled reaction in the nickel foam is about 10^5 A cm mol^{-1} and the comparison again confirms that the oxidation of alcohols is fully controlled by the kinetics of a surface chemical reaction.

Sets of I–E curves were recorded for several concentrations of ethanol at the full sized twin grid, foam and stacked net electrodes. As in the case of the smaller foam electrode discussed above, the I–E responses showed ethanol oxidation to occur in the expected potential range but well-formed waves were not observed. It should be emphasized that the poor plateaux are specific to alcohol oxidation and, as noted earlier, good mass transport limited plateaux were observed at all materials for the reduction of ferricyanide. The limiting rates of ethanol oxidation were therefore estimated by measuring the currents at +0.44 V (with allowance for the background current in the absence of ethanol) and in all cases the j_L against c plots were linear. Assuming that the rate of ethanol oxidation at the various nickel surfaces is the same, the relative values of the slopes of the j_L against c plots for ethanol at the three dimensional electrodes and the flat plate anode allow an estimate of the surface area of nickel in 1 cm^2 of each electrode material. Allowing for the thickness of each electrode material, their specific surface areas may then be estimated. The values found are reported in Table 4.

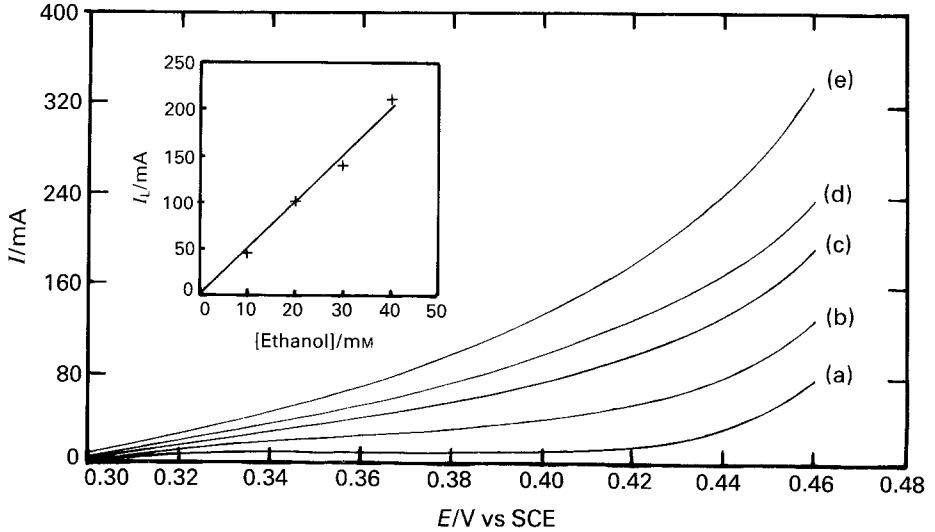

Fig. 6. I–E curves for ethanol in 1 M KOH at a 2 cm × 4 cm piece of nickel foam anode. Potential scan rate 1 mV s^{-1}. Ethanol concentrations: (a) 0; (b) 25; (c) 50; (d) 75; and (e) 100 mM. The inset shows the relationship between the current at +0.44 V and the concentration of ethanol.

Table 4. Reports on (a) the values of j_L/c for the oxidation of ethanol at the different extended area electrodes; (b) the estimates of A_e obtained by comparing I_L/c with the value of the flat plate electrode; (c) the values of k_LA_e (at $v = 9\,cm\,s^{-1}$) for the same materials from the studies on the reduction of ferricyanide; and (d) the values of k_L obtained by dividing k_LA_e by A_e.

	j_L/c^* /A cm mol^{-1}	A_e /cm^{2}cm^{-3}	$10^3k_LA_e$ /s^{-1}	10^3k_L /cm s^{-1}
Flat plate	6	–	–	2.0
Twin grid	19	8	22	2.8
Stacked net	108	36	188	5.2
Metal foam	105	44	88	2.0

* Measured at +0.44 V.

The value of A_e for the nickel foam is within the range for similar foam materials reported in earlier papers [22,23]. This method of estimating A_e is subject to errors due to the difference in the activity of various nickel surfaces for ethanol oxidation. The data for the polished disc and flat plate electrodes described above is perhaps a good guide to likely errors and the estimates of A_e are reliable to within a factor of two. The method does, however, provide an alternative to pressure drop measurements where uncertainties of a similar magnitude can arise.

Table 4 also reports values of k_LA_e and the values of k_L obtained by division of k_LA_e by A_e. The values confirms that the twin grid electrode is a reasonable turbulence promoter and the stacked net is a very efficient turbulence promoter. This would be predicted from the results with polymer promoters of comparable structure [13]. The comparison of k_L and A_e for the stacked net and foam electrodes is interesting. The good performance of the stacked nets arises largely from their ability to enhance turbulence but that at the foam is more the result of a very high area. This is, perhaps a surprising conclusion but it is consistent with the results from another study in our laboratories [24]. Indeed, in this set of experiments, the foam electrode in the FM01 cell appears not to be a significant turbulence promoter. This result may, however, partly again arise from differences in the activity of the nickel surfaces for alcohol oxidation (or oxygen evolution). The results are consistent with the nickel foams having a particularly high activity for alcohol oxidation and this could arise, for example, if the nickel of the foam has a lower purity.

For the preparative scale oxidation of alcohols, it is A_e which is critical and, therefore, these results, together with its greater robustness and ease of use compared with the stacked net, that led to the use of a metal foam for preparative experiments.

3.5. *Preparative scale electrolyses*

Preliminary electrolyses were carried out at constant potential in the FM01 cell fitted with the single sheet nickel foam anode (16 cm × 4 cm × 0.4 cm) and a flat plate nickel cathode. The anode potential was +0.42 V vs SCE and the solutions contained 35 mmol of the alcohols in 350 cm^3 of 1 M KOH; the electrolysis was continued until a charge equivalent to 4e$^-$/molecule of the alcohol had been passed. After electrolysis of the ethanol solution, the analysis showed the formation of 28 mmol of ethanoic acid and some 6 mmol of ethanol remaining. Hence, the electrolysis occurred with very good selectivity and a reasonable current yield; the initial cell current was 820 mA and the electrolysis was complete in 7 h. The selectivities and current efficiencies from the electrolyses with propanol and butanol were similar but the reactions took longer as the initial currents were only 380 and 170 mA, respectively. The electrolyses had to be carried out in a divided cell (using a Nafion^{TM} 324 membrane) because, with an undivided cell, hydrogen from the counter electrode collected in the Luggin capillary and caused the cell potential to oscillate.

Therefore, further electrolyses were carried out in an undivided cell but employing a constant current. With a cell current of 0.5 A for 4 h, the oxidation of ethanol, propanol and butanol gave current efficiencies of 86%, 80% and 67%, respectively. Determination of the remaining alcohols suggested that the selectivities approached 100%. Thus, the constant current procedure provided an effective way of converting about 20 mmol of alcohol to the carboxylic acid in some 4 h. At a flat plate electrode, the same production rate requires a cell with approaching 1 m^2 of anode! The FM01-LC electrolyser with a nickel foam electrode is, therefore, a convenient laboratory material for the synthesis of carboxylic acids while larger cells with nickel foam anodes could be constructed for the scale-up of such syntheses. The failings of smooth anodes to give an acceptable rate of conversion has long been recognised and earlier attempts to overcome the problem have been based on the preparation of rough surfaces [25–27] and modified catalysts [28,29]. None are as effective and convenient as the use of the nickel foam electrode.

A recent paper [30] has described the anodic oxidation of isopropylideneglycerol to the corresponding carboxylic acid which was then converted to its ester, methyl isopropylideneglycerate,

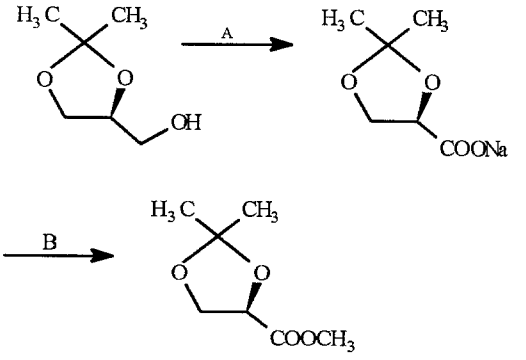

which is a versatile intermediate for the synthesis of chiral lipids; the isopropylidene group is a common protecting group for diols. The electrolysis employed a silver anode in aqueous hydroxide and while it

gave a good yield, it took 56 h to complete. In view of the similarity in the mechanism of operation of silver and nickel anodes in base [16], this reaction was considered a good test of the FM01 reactor with a nickel foam anode.

Preliminary experiments with a nickel disc electrode confirmed that a solution of isopropylideneglycerol in 1 M NaOH gave the expected well formed oxidation wave, $E_{1/2} = 0.39$ V and a relatively high limiting current density (equivalent to 20.4 A cm mol^{-1}), proportional to the concentration of isopropylideneglycerol. Preparative scale electrolysis was performed in an undivided cell, employing a cell current of 0.56 A. The electrolyte consisted of 300 cm^3 of 0.1 M isopropylideneglycerol in 1.0 M NaOH, thermostatted at 298 K. After the passage of a charge equivalent to 4e$^-$/molecule (taking approximately 5.5 h), the yield of organic acid, as determined by the resin neutralisation and titration procedure, was 60% and the unconverted alcohol, determined by gas chromatography, was 35%. Hence, the reaction appears to have an excellent selectivity and reasonable current efficiency and the conversion is achieved at an acceptable rate for a laboratory synthesis.

It was considered important to confirm the identity of the product. Attempts to isolate the carboxylic acid, for example, using the resin neutralisation method to remove the Na^+ ions from solution were unsuccessful. NMR spectroscopy confirmed the tendency for the isopropylidene protecting group to undergo rapid acid hydrolysis if the pH dropped below 5 (note that this hydrolysis does not affect the quantity of acid groups available for titration and, hence, does not invalidate the analysis described above). Instead, a literature procedure [30] was used to isolate crystals of the sodium salt of the carboxylic acid. This was a white crystalline solid, melting point of 249–253 °C and it showed the following spectroscopic characteristics:

$$^1\text{H NMR } (D_2O) : \delta = 1.40(\text{s}, 3\text{H}, CH_3),$$
$$1.45(\text{s}, 3\text{H}, CH_3), 3.62(\text{m}, 1\text{H}, CH_2),$$
$$4.30(\text{m}, 1\text{H}, CH_2), 4.50(\text{m}, 1\text{H}, CH).$$
$$\text{IR(KCl)} : \nu = 2920\,\text{cm}^{-1}(CH_3), 1600(COO^-),$$
$$1450(COO^-), 1360(C(CH_3)_2)$$

which agreed fully with the literature [30]. The isolated yield was only 21% but no evidence was found for other products. Indeed, in all experiments, the only other product observed arose from hydrolysis of the protecting group. This synthesis demonstrates the utility of the cell with a three dimensional electrode for organic reactions of real interest in synthesis.

4. Conclusion

It has been shown that the FM01-LC electrolyser is readily modified to allow the incorporation of stationary, flow-by, three-dimensional electrodes; for reactions which occur only at low current densities, this allows the rate of conversion to be enhanced by a factor up to one hundred. Several types of three dimensional electrodes have been characterized and compared by determining $k_L A_e$ from the mass transport controlled limiting current for the reduction of ferricyanide as a function of electrolyte flow rate. It has also been shown that the determination of the kinetically controlled limiting current for the oxidation of an alcohol at nickel allows an estimate of A_e, based on quite different concepts to the normal method based on pressure drop measurements.

A particularly convenient type of such electrode with high specific area is fabricated from metal foam. The oxidation of alcohols to carboxylic acids at a nickel anode in aqueous base are selective reactions of interest in synthesis but have the drawback that they occur only at very low current densities; with a nickel foam anode, the FM01-LC cell allows these reactions to be carried out at an acceptable rate and therefore enhances the applicability of these reactions.

Acknowledgement

The authors would like to express their gratitude to ICI Chemicals & Polymers Limited for financial support of this programme.

References

[1] J. S. Newman and W. Tiedeman, *Adv. Electrochem. & Electrochem. Engng.*, **11** (1978) 353.
[2] F. Coeuret, *J. Appl. Electrochem.* **10** (1980) 687.
[3] G. Kreysa, *Metalloberflache* **35** (1981) 6.
[4] R. E. Sioda and K. B. Keating, *Electroanal. Chem.* **12** (1982) 1.
[5] F. Goodridge and A. R. Wright, *in* 'Comprehensive Treatise of Electrochemistry', Vol. 6', (edited by J.O'M. Bockris, B. E. Conway, E. Yeager and R.E. White), Plenum, London (1983) p. 393.
[6] B. Fleet, *Coll. Czech Chem. Comm.* **53** (1988) 1107.
[7] D. Pletcher and F. C. Walsh, *in* 'Electrochemical Technology for a Cleaner Environment, (edited by J. D. Genders and N.L. Weinberg), The Electrosynthesis Co., Lancaster, NY. (1992) p. 51.
[8] D. Pletcher and F. C. Walsh, Industrial Electrochemistry, Chapman & Hall, London (1990).
[9] D. Pletcher, I. Whyte, F. C. Walsh and P. J. Millington, *J. Appl. Electrochem.* **21** (1991) 659.
[10] D. Simonsson, *J. Appl. Electrochem.* **14** (1984) 595.
[11] D. Robinson, *in* 'Electrosynthesis – from Laboratory, to Pilot, to Production', (edited by J. D. Genders and D. Pletcher), The Electrosynthesis Co., Lancaster, NY. (1990) p. 219.
[12] C. J. Brown, D. Pletcher, F. C. Walsh, J. K. Hammond and D. Robinson, Dechema monographs, 'Electrochemical Cell Design and Optimisation Procedures', 123, (1991) p. 299.
[13] C. J. Brown, D. Pletcher, F. C. Walsh, J.K. Hammond and D. Robinson, *J. Appl. Electrochem.* **23** (1993) 38.
[14] C. J. Brown, D. Pletcher, R. C. Walsh, J. K. Hammond and D. Robinson, *ibid.* **22** (1992) 613.
[15] M. Fleischmann, K. Korinek and D. Pletcher, *J. Electroanal. Chem.* **31** (1971) 39.
[16] *Idem, J. Chem. Soc. Perkin II* (1972) 1396.
[17] P. M. Robertson, *Electrochim. Acta* **22** (1977) 411.
[18] H. J. Schäfer, *Topics in Current Chemistry* **141** (1987) 101.
[19] F. Leroux and F. Coeuret, *Electrochim. Acta* **30** (1985) 159.
[20] S. Langlois and F. Coeuret, *J. Appl. Electrochem.* **19** (1989) 51.

[21] F. Leroux and F. Coeuret, *Electrochim. Acta* **30** (1985) 167.
[22] S. Langlois and F. Coeuret, *J. Appl. Electrochem.* **19** (1989) 43.
[23] D. Pletcher, I. Whyte, F. C. Walsh and J. P. Millington, *J. Appl. Electrochem.* **21** (1991) 659.
[24] G. W. Reade and F. C. Walsh, unpublished results.
[25] G. Vertes, G. Horanyi and F. Nagy, *Tetrahedron* **28** (1972) 37.
[26] K. Manandhar and D. Pletcher, *J. Appl. Electrochem.* **9** (1979) 707.
[27] P. M. Robertson, P. Berg, H. Reimann, K. Schleich and P. Seiler, *J. Electrochem. Soc.* **130** (1983) 591.
[28] P. Cox and D. Pletcher, *J. Appl. Electrochem.* **20** (1990) 549.
[29] *Idem, ibid.* **21** (1991) 11.
[30] K. H. Schwarz, K. Kleiner, R. Ludwig, E. Schrötter and H. Schick, *Liebigs. Ann. Chem.* (1991) 503.